ASEG-PESA 2015
Geophysics and Geology together for Discovery
24th International Geophysical Conference and Exhibition
15 – 18 February 2015 Perth, Western Australia

Horizontal resolution of seismic acquisition geometries

Wei Wei
Institute of Geology and Geophysics
Chinese Academy of Sciences
No. 19, Beitucheng Xilu
Chaoyang District, Beijing, China
E-mail: caswei@gmail.com

Li-Yun Fu
Institute of Geology and Geophysics
Chinese Academy of Sciences
No. 19, Beitucheng Xilu
Chaoyang District, Beijing, China
E-mail: lfu@mail.iggcas.ac.cn

Weijia Sun
Institute of Geology and Geophysics
Chinese Academy of Sciences
No. 19, Beitucheng Xilu
Chaoyang District, Beijing, China
E-mail: swj@mail.iggcas.ac.cn

SUMMARY

Spatial sampling has a crucial influence on the horizontal resolution of seismic imaging, but how to quantify the influence is still controversial especially in complex media. Most of the studies on horizontal resolution focus on the measurement of wavelet widths for seismic migration, but neglect to evaluate the effect of side-lobe perturbations on spatial resolution. The side-lobe effect, as a migration noise, is important for seismic imaging in complex media. In this article, with focal beam analysis, we define two parameters to represent the horizontal resolution of an acquisition geometry: the width of the main lobe (WML) along the inline and crossline directions and the ratio of the main-lobe amplitude to the total amplitude (RMT) in a focal beam. We provide examples of typical acquisition geometries to show that how spatial sampling affects the horizontal resolution, measured in terms of WML and RMT values. WML defines the horizontal resolution to image the target, whereas RMT describes the clarity of the imaging. Migration noise reduces with increasing RMT, indirectly improving both the vertical and horizontal resolutions of seismic imaging. Case studies of seismic migration with 3D seismic data demonstrate how the acquisition geometries with different WML and RMT values influence the performance of seismic imaging. A prior WML and RMT analysis to predict the quality of acquired datasets can optimize acquisition geometries before the implementation of seismic acquisition.

Key words: seismic acquisition geometry; spatial resolution; focal beam; complex media; migration noise.

INTRODUCTION

Spatial resolution has been extensively studied by various articles on prestack migration and inversion (e.g., Berkhout, 1984). Since 1990s, the methodology for spatial resolution analysis has been established in various articles; for instance, spatial resolution analysis (Vermeer, 1999; Gibson and Tzimeas, 2002) based on the theory of Beylkin (1985) and illumination analysis (Xie et al., 2006) in terms of the local plane-wave. In contrast to spatial resolution analysis, focal beam analysis (Berkhout et al., 2001; Volker et al., 2001) directly relates prestack migration to the assessment of seismic acquisition geometries, by which we can analyze the detector and source parts of acquisition geometry, separately. Volker's formulations are applicable to both homogeneous and heterogeneous media (Volker et al., 2001). Van Veldhuizen et al. (2008) developed a model-based implementation of the focal beam analysis method for inhomogeneous media in the space-frequency domain. Wei et al. (2012) proposed a rapid multi-frequency focal beam method in the frequency-wavenumber domain. However, most of these studies only focus on the measurements of wavelet widths for seismic migration, with an assumption of the side-lobe effect or migration noise on spatial resolution indirectly. The effect of side lobes is a very critical component to imaging for complex structures under realistic situations in deed. Berkhout (1984) pointed out that spatial resolution is determined by not only the main lobe of wavelet but also the sidelobe strength relative to the main lobe. In complex media, such as salt dome structures, igneous rocks, steep structures, and fracture zones, the propagation effect of seismic wavefields caused by lateral variations in velocity on structural imaging, further reduces the peak-to-sidelobe ratio of spatial resolution by increasing the variance.

In this article, we review focal beam method and define two parameters to represent the horizontal resolution: the width of the main lobe (WML) along the inline or crossline directions and the ratio of the main-lobe amplitude to the total amplitude (RMT). Several examples of typical acquisition geometries demonstrate that the spatial sampling has a significant impact on the spatial resolution, measured in terms of WML and RMT values. Finally, the WML and RMT analysis is applied to a 3D model demonstrating how the difference of spatial sampling or velocity model affects horizontal resolution of seismic imaging. Case studies with the comparison between different acquisition geometries show that the performance of seismic imaging is largely affected by the WML and RMT values. A prior WML and RMT analysis for a selected acquisition scheme is an excellent way to predict the quality of acquired datasets before the implementation of seismic acquisition.

METHOD

The focal beam analysis method (Berkhout et al., 2001; Volker et al., 2001) originates from the migration of seismic reflection data using the common focus-point concept (Berkhout, 1997). As described in Berkhout et al. (2001), double-focusing migration yields the following spatial resolution matrix

$$\mathbf{B}(z_m, z_m) = \mathbf{B}_D(z_m, z_0)\mathbf{B}_S(z_0, z_m) , \tag{1}$$

where $\mathbf{B}_D(z_m,z_0)$ and $\mathbf{B}_S(z_0,z_m)$ are the focal-detector and focal-source matrices, respectively. Note that in the ideal case, $\mathbf{B}(z_m,z_m)$ is an identity matrix $\mathbf{I}(z_m,z_m)$. $\mathbf{B}(z_m,z_m)$ quantifies, however in practice, the imprint of acquisition geometry on the reflectivity information, caused by the sparse sampling of sources and detectors.

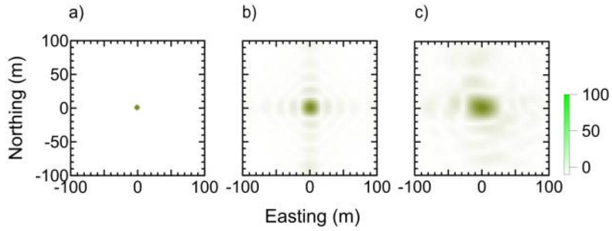

Figure 2. Comparison of the focal beams between the ideal case (a), the case (b) in homogenous media, and the actual case (c) in complex media for the target point at (x,y) = (0,0).

In order to describe the vertical resolution, Schoenberger (1974) defined a peak-to-sidelobe ratio between the central-peak amplitude and the sidelobe amplitude. Koefoed (1981) proposed three factors that control the vertical resolution: (1) the width of the main lobe, (2) the side lobe ratio or peak-to-trough ratio, and (3) the amplitude of oscillations. These studies on the vertical resolution can be also applicable to describe the horizontal resolution. As shown in Figure 1, in the ideal case, the spatial resolution function of focal beams will peaks (Figure 1a) at the location of the target point (Van Veldhuizen, 2008). However in practice, because of discrete process and finite-length sampling it always has a wider peak with obvious sidelobe noises (Figure 1b) even for a homogeneous medium. In complex media, the effect of lateral variations in velocity on seismic imaging further reduces the peak-to-sidelobe ratio of spatial resolution by increasing the variance (Figure 1c). As shown in Figure 2, we use two parameters to represent the horizontal resolution: the width of the main lobe (WML) along the inline or crossline directions and the ratio of the main-lobe amplitude to the total amplitude (RMT). WML defines the horizontal resolution for the imaging of the target, whereas RMT describes the clarity of the imaging. The migration noise reduces with increasing RMT, indirectly improving both the vertical and horizontal resolutions of seismic imaging.

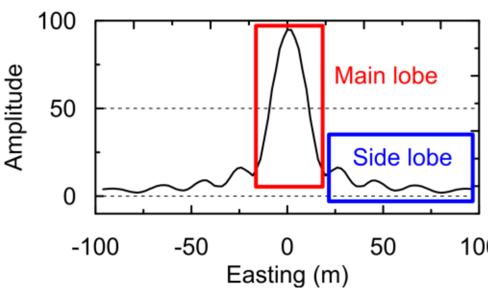

Figure 2: Inline section of focal beam. Two parameters are used to quantify the lateral resolution: the width of the main lobe (WML) and the ratio of the main-lobe amplitude to the total amplitude (RMT).

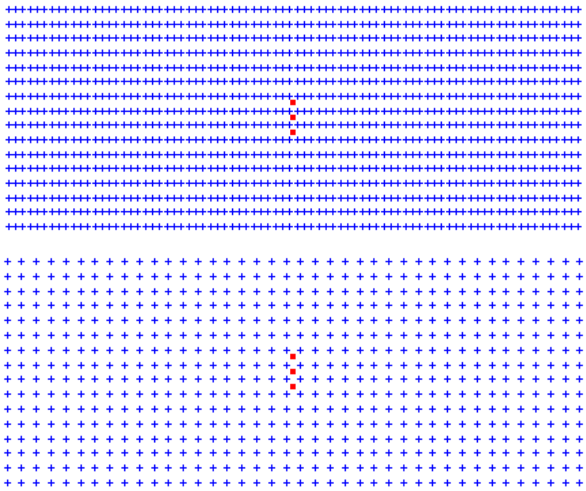

Figure 3. Two orthogonal acquisition templates each consist of 16 detector lines with 4000 m in length. Scheme I (upper panel) is the original acquisition geometry to be implemented actually, and Scheme II (lower panel) is a half-detector-density version simplified from Scheme I. The square represents sources and the cross indicates detectors.

CASES STUDIES

We apply focal beam analysis to different acquisition geometries. As shown in Figure 3, two orthogonal acquisition templates, each consisting of 16 detector lines with 4000 m in length, are exampled as Schemes I and II. Scheme I is the original acquisition geometry that has been implemented actually in seismic exploration, with 50-m detector interval, 100-m source interval, 100-m detector-line spacing, and 100-m source-line spacing. Scheme II is a half-detector-density version simplified from Scheme I, with 100-m detector interval, 100-m source interval, 100-m detector-line spacing, and 100-m source-line spacing. Both the geometry templates are rolled during the acquisition totally 20 times longitudinally with each time the same inline-rolling distance 100 m, and 3 times transversely with each time the same crossline-rolling distance 400 m. The resulting full folds (160) are the same for both the acquisition schemes. The focal beam analysis of both the schemes is conducted for a frequency range of 10-35 Hz with a dominant frequency of 20 Hz.

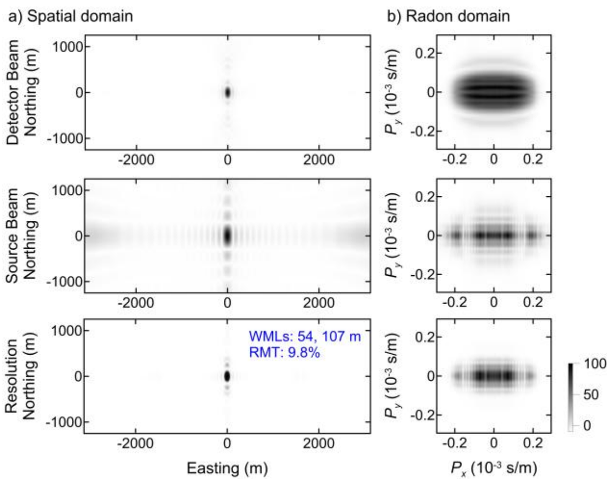

Figure 4. Focal beams of Scheme I for a homogeneous medium with a target depth of 2313 m. (a) Detector beam, source beam, and resolution function in the spatial domain. (b) The corresponding versions in the Radon domain. The colors indicate the amplitudes on a linear scale. Resulting inline width of the main lobe (inline WML), crossline width of the main lobe (crossline WML) and the ratio of the main-lobe amplitude to the total amplitude (RMT) is 54 m, 107 m and 9.8%, respectively.

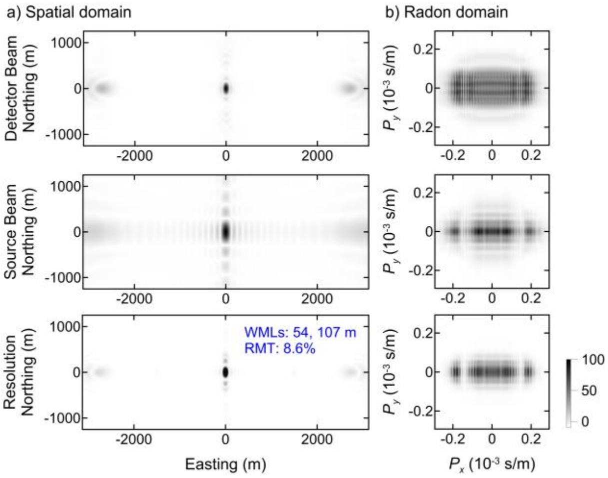

Figure 5. Focal beams of Scheme II for a homogeneous medium with a target depth of 2313 m. (a) Detector beam, source beam, and resolution function in the spatial domain. (b) Resulting inline width of the main lobe (inline WML), crossline width of the main lobe (crossline WML) and the ratio of the main-lobe amplitude to the total amplitude (RMT) is 54 m, 107 m and 8.6%, respectively.

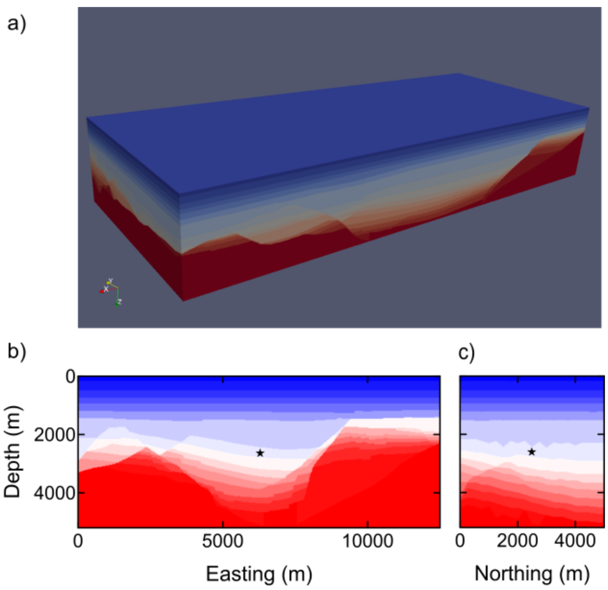

Figure 6. A 3D velocity model (a) and its two lateral sections (b). The model, with a total dimension of 12.5 (x) × 5 (y) × 5.2 km (z), contains a number of layers with complex fault structures. Velocities vary from 2100.0 m/s in the topmost layer to 5500.0 m/s in the bottom layer. The target point is located at the point (3125.0, 1250.0, 2313.0) m (indicated by star in the figure).

We first test these schemes for a homogeneous medium with a target depth of 2313 m. The resulting spatial resolution function, the focal-detector and focal-source beams, and the corresponding radon-domain versions, i.e., the amplitude imprints versus ray parameter (AVP) imprints, are shown in Figures 4 and 5, respectively. We see that the main lobes of the detector and source beams and the spatial resolution function are almost the same between Schemes I and II in the space domain, implying that both the schemes have a similar spatial resolution. That is, the WMLs of Schemes I and II are almost the same, leading to a similar spatial resolution for seismic imaging. However, Scheme II with a sparser detector spacing presents stronger side-lobe perturbations than Scheme I, involved with heavier aliasing effects along the easting (inline) direction. That is, Scheme II has a lower RMT value, causing a poor spatial clarity for seismic imaging. On the other hand, Scheme I with a denser detector interval shows a more uniform distribution of the AVP imprints along the easting (inline) direction than Scheme II, leading to more concentrated energy responses and uniform angle-dependent amplitudes at the target point along the inline direction.

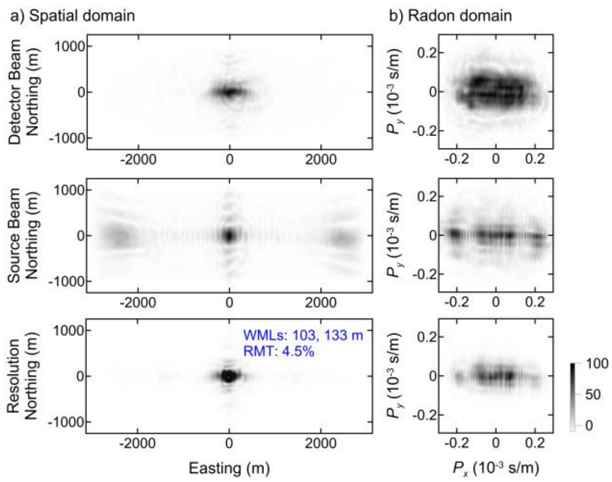

Figure 7. Focal beams of acquisition Scheme I at depth 2313 m for the velocity model shown in Figure 10. (a) Detector beam, source beam, and resolution function in the spatial domain. (b) The corresponding versions in the Radon domain. The colors indicate the amplitudes on a linear scale. Resulting inline width of the main lobe (inline WML), crossline width of the main lobe (crossline WML) and the ratio of the main-lobe amplitude to the total amplitude (RMT) is 103 m, 133 m and 4.5%, respectively.

We example these schemes for heterogeneous media using a velocity model shown in Figure 6. The model-based focal beam analysis is conducted for Schemes I and II, as shown in Figures 7 and 8, respectively. We see that in contrast to the focal beams in homogeneous media shown in Figures 4 and 5, the main-lobe energy of the focal beams in heterogeneous media becomes disperse, with much large WMLs. That is, for seismic imaging in complex media, the effect of lateral velocity variations on wavefields will impairs the WML and RMT of an acquisition geometry by increasing the variance. Similar to the case of homogeneous medium, Schemes I and II have a similar spatial resolution for seismic imaging in heterogeneous media because of almost the same WMLs between two Schemes. Strong side-lobe perturbations can be seen in the focal beams of Scheme II with a sparser detector spacing, which reduce its RMT, cause heavier aliasing effects along the easting (inline) direction, and impair the spatial clarity of seismic imaging. On the other hand, some uniform distribution of the AVP imprints along the easting (inline) direction can be seen in the focal beams of Scheme I with a denser detector spacing, leading to more concentrated energy responses and uniform angle-dependent amplitudes for imaging the target point along the inline direction. In conclusion, denser detector spacing almost does not affect the spatial resolution of an acquisition geometry, but significantly improve the spatial clarity of seismic imaging by less aliasing effects, more concentrated energy responses, and more uniform angle-dependent amplitudes along the inline direction. These mechanisms of action, as an advantage in a prior analysis of acquisition geometries, can be described by the WML and RMT of focal beams to measure the performance of acquisition geometries for seismic imaging.

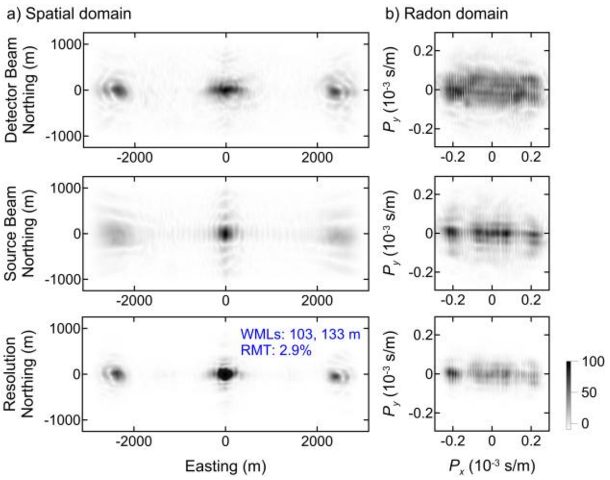

Figure 8. Focal beams of acquisition Scheme II at depth 2313 m for the velocity model shown in Figure 10. (a) Detector beam, source beam, and resolution function in the spatial domain. (b) The corresponding versions in the Radon domain. The colors indicate the amplitudes on a linear scale. Resulting inline width of the main lobe (inline WML), crossline width of the main lobe (crossline WML) and the ratio of the main-lobe amplitude to the total amplitude (RMT) is 103 m, 133 m and 2.9%, respectively.

CONCLUSIONS

We review focal beam method and define two parameters to represent the horizontal resolution: the width of the main lobe (WML) along the inline or crossline directions and the ratio of the main-lobe amplitude to the total amplitude (RMT). WML defines the horizontal resolution for the imaging of the target, whereas RMT describes the clarity of the imaging. The migration noise reduces with increasing RMT, indirectly improving both the vertical and horizontal resolutions of seismic imaging. The focal beam method is applied to a case study with two acquisition geometries of different detector sampling densities for 3D seismic acquisition in an oilfield. The resulting WMLs of two acquisition schemes are almost the same, leading to a similar spatial resolution for seismic imaging. However, acquisition scheme with sparser detector density has a lower RMT value, causing a poor spatial clarity for seismic imaging. On the other hand, compared with focal beam in homogeneous media, model-based focal beams in heterogeneous media have disperser main-lobe energy with much large WMLs. That is, for imaging in complex media, the effect of lateral velocity variations on wavefields will impairs the WML and RMT of acquisition geometries by increasing the variance. These mechanisms of action, as an advantage in a prior analysis of acquisition geometries, can be described by the WML and RMT of focal beams to measure the performance of acquisition geometries for seismic imaging.

ACKNOWLEDGMENTS

The research was supported by the Natural Science Foundation of China (Grant Nos. 41204098 and 41130418).

REFERENCES

Berkhout, A. J., 1984. Seismic resolution: a quantitative analysis of resolving power of acoustical echo techniques: Geophysical Press, London – Amsterdam.

Berkhout, A. J., 1997. Pushing the limits of seismic imaging, Part I: Prestack migration in terms of double dynamic focusing: Geophysics, 62, 937-953.

Berkhout, A. J., L. OngKiehong, A. W. F. Volker, and G. Blacquiere, 2001. Comprehensive assessment of seismic acquisition geometries by focal beams—Part I: Theoretical considerations. Geophysics, 66: 911~917.

Beylkin, G., 1985. Imaging of discontinuities in the inverse scattering problem by inversion of a causal generalized Radon transform: Journal of Mathematical Physics, 26, 99-108.

Gibson, R. L. and C. Tzimeas, 2002. Quantitative measures of image resolution for seismic survey design: Geophysics, 67, 1844-1852.

Koefoed, O., 1981. Aspects of vertical seismic resolution: Geophysical Prospecting, 29, 21-30.

Schoenberger, M., 1974. Resolution comparison of minimum-phase and zero-phase signals: Geophysics, 39(6), 826–833.

Van Veldhuizen, E. J., G. Blacquière, and A. J. Berkhout, 2008. Acquisition geometry analysis in complex 3D media: Geophysics, 73, Q43-Q58.

Vermeer, G. J. O., 1999. Factors affecting spatial resolution: Geophysics, 64, 942-953.

Volker A W F, G. Blacquiere, A. J. Berkhout, and L. OngKiehong, 2001. Comprehensive assessment of seismic acquisition geometries by focal beams—Part II: Practical aspects and examples. Geophysics, 66: 918~931.

Wei, W., L. Y. Fu and G. Blacquière, 2012. Fast multifrequency focal beam analysis for 3D seismic acquisition geometry: Geophysics, 77, P11-P21.

Xie, X. B., and R. S. Wu, 2006. Wave-equation-based seismic illumination analysis: Geophysics, 71(5), S169-S17